LWT - Food Science and Technology 174 (2023) 114411

Contents lists available at ScienceDirect

LWT

journal homepage: www.elsevier.com/locate/lwt

Characterization of sulfur compounds and antiviral activity against *Tomato brown rugose fruit virus* (ToBRFV) of Italian "Vessalico" garlic compared to other cultivars and landrace

Valeria Iobbi [a,1], Valentina Santoro [b,1], Norbert Maggi [c], Mauro Giacomini [c], Anna Paola Lanteri [d], Giovanni Minuto [d], Andrea Minuto [d], Paola Fossa [a], Nunziatina De Tommasi [b,**], Angela Bisio [a,*], Giuliana Drava [a]

[a] Department of Pharmacy, University of Genova, Viale Cembrano 4, 16145, Genova, Italy
[b] Department of Pharmacy, University of Salerno, Via Giovanni Paolo II 132, 84084, Salerno, Italy
[c] Department of Informatics, Bioengineering, Robotics and System Science, University of Genova, Via Opera Pia 13, 16145, Genova, Italy
[d] CERSAA Centro di Sperimentazione e Assistenza Agricola, Regione Rollo 98, 17031, Albenga, Italy

ARTICLE INFO

Keywords:
Anti-ToBRFV activity
Garlic
Multivariate analysis
UHPLC-QTOF-MS
Vessalico garlic

ABSTRACT

In this study the Italian garlic "Aglio di Vessalico" was compared with the French cultivars Messidrôme and Messidor, whose cloves are used every year by the growers of Vessalico (Imperia, Italy) for sowing, and with the geographically adjacent "Aglio di Caraglio". UHPLC-Q-trap analyses of the extracts of these commercial garlic accessions showed similar profiles for sulfur compounds, highlighting the presence of typical molecules of stored garlic. HC, PCA and SOM, applied to the LC/MS data, allowed to separate the garlic accessions, confirming similarities between Vessalico and French accessions, while Caraglio formed a more compact group. All garlic extracts showed ability to deactivate *Tomato brown rugose fruit virus* (ToBRFV) infectivity, as a possible consequence of disassembly of the virus coat protein (CP). Molecular docking showed a strong interaction of the sulfur compounds characteristic of aged extracts with a high number of residues into ToBRFV CP binding site, interfering with virulence progress.

1. Introduction

Garlic (*Allium sativum* L.) is a food known worldwide as economically significant vegetable for its aroma and health benefits. The chemistry of garlic has been deeply studied, and non-polar compounds, such as thiosulfinate and sulfur compounds, as well as relative polar compounds, such as (poly)phenols, anthocyanins, flavonoids, carotenoids, phytosterols, and saponins, many of which glycosylated, have been reported (Block, 2010; Lanzotti, 2012). Garlic shows a high biodiversity, environmental-adaptation capacity, and phenotypic plasticity with variation for several morphological and chemical aspects (Volk, 2009). Consequently, many varieties or cultivars of garlic are available, that can be selected and identified based on morphological, biochemical and DNA data (Ipek, Ipek, & Simon, 2003). Multiple agricultural ecotypes, as a consequence of local adaptation (Lakoba & Barney, 2020), have been also described (Benke et al., 2021), and the variability of sulfur compounds in garlic ecotypes from different geographical regions has been reported (González, Soto, Sance, Camargo, & Galmarini, 2009).

A number of garlic varieties, farmers' varieties, cultivars, and landraces are used in Italy for commercial cultivation and several of them are listed in the "National List of Traditional Agri-Food Products" of the Ministry of Agricultural, Food and Forestry Policies (MIPAAF, 2021). "Aglio bianco (di Vessalico)" ("Aglio di Vessalico", Vessalico white garlic) (MIPAAF, 2021) is one of the best known Italian garlics, whose geographical area of cultivation, processing, and packaging is located in Valle Arroscia (Imperia, Italy). Due to its obligate apomictic nature, garlic is reproduced almost exclusively by means of cloves or vegetative topsets in the inflorescence (Pooler & Simon, 1994). Vessalico garlic is reproduced every year by cloves belonging to the French cultivars Messidrôme and Messidor (GEVES, 2015b). Both Messidrôme and

* Corresponding author.
** Corresponding author.
E-mail addresses: detommasi@unisa.it (N. De Tommasi), angela.bisio@unige.it (A. Bisio).
[1] **Valeria Iobbi** and **Valentina Santoro** contributed equally to this paper.

https://doi.org/10.1016/j.lwt.2022.114411
Received 7 July 2022; Received in revised form 27 December 2022; Accepted 29 December 2022
Available online 31 December 2022

Messidor are included into garlic variety group III, "Blancs de la Drôme" type (Messiaen, Cohat, Leroux, Piechon, & Beyries, 1993). Variety group III comprises cultivars from southern Europe, with large bulbs without flowering stems and large cloves. Messidor is distinguished from Messidrôme by a darker and higher foliage (GEVES, 2015a). The bulb of Vessalico garlic is smaller than those of the parent cultivars, white in colour, with pink to purple streaked tunics. The bulb consists of several white bulblets or cloves (6–14), and it is roundish, regular, compact, and slightly flattened at the point of insertion of the root system. The area of cultivation of Vessalico garlic is quite close to the area of the landrace Caraglio garlic ("Aglio di Caraglio") (MIPAAF, 2021), characterized by a small bulb with tapered segments showing deep red streaks. At present a characterization of Vessalico garlic as an agricultural ecotype, as well as a sustainable exploitation of this local crop has not yet been made. As soil and climate conditions, as well as cultivation and storage practices in different locations (Martins, Petropoulos, & Ferreira, 2016), are known to affect the chemical composition and the quality of the final product, LC/MS metabolite profiling together with multivariate statistical techniques were applied to chemically characterize Vessalico garlic compared to the French parent cultivars Messidrôme and Messidor, and to Caraglio garlic. Moreover, to find new possibilities for the use of production waste and residues from the sales of marketed bulbs, in this study the extracts of the commercial cloves of these garlic types were investigated as possible agrochemicals. As a matter of fact, the use of local crops to produce total extracts or phyto-constituents to be used in organic farming or in integrated pest management systems is at present a challenge in terms of sustainable territorial development (European Commission, 2020; European Parliament, 2009). The pesticide industries look with interest to extracts and compounds of natural origin that can be used both in integrated and in organic agriculture (Godlewska, Ronga, & Michalak, 2021). In this scenario the research of plant products active as antivirals to be used in agriculture is of relevance, since few extracts revealed this type of bioactivity till now (Bhyan, Alam, & Ali, 2007; Hamidson, Damiri, & Angraini, 2018; Islam, Adnan, Tayyab, Hussain, & Islam, 2018). Plant sulfur compounds are involved in plant defence responses to pathogens (Künstler, Gullner, Ádám, KolozsvárinéNagy, & Király, 2020) and garlic extracts showed antiviral activity against plant infections (*Potato virus Y*, *Tomato spotted wilt virus*, *Grapevine leafroll virus*) (Rouf et al., 2020). At present no information is available about the antiviral activity of garlic extracts against *Tomato brown rugose fruit virus* (ToBRFV), a *Tobamovirus* that affects tomato crops and poses a serious threat to their profitable production (EPPO, 2022).

Tomato (*Solanum lycopersicum* L.) is one of the most widely grown and economically important vegetable crops in the world. Italy is among the top ten tomato producers worldwide and is the most important EU producer, with an annual production in 2020 of about six million tons (Eurostat, 2022). However, tomato is particularly susceptible to viral disease infections, with hundreds of viruses in 40 recognized genera infecting solanaceous plants and drastically reducing the yield and quality of tomato crops. *Tobamovirus* is the largest genus of the *Virgaviridae* family that affects tomato crops and poses a serious threat to the profitable production of this vegetable. *Tobacco mosaic virus* (TMV) is one of the most important species of *Tobamovirus* infecting tomatoes, and it is widely used as a model to study host-pathogen interaction and virus evolution (Scholthof, 2004). ToBRFV is a new member of the *Tobamovirus* genus. This virus was first reported in 2016 from tomato plants grown in greenhouses in Jordan in 2015 and subsequently in other countries in Europe, North America and China, thus rising dissemination of *Tobamovirus* outbreaks at global level. In January 2019 ToBRFV was added to the EPPO Alert List, and subsequently in 2020 to the EPPO A2 List of pests recommended for regulation as quarantine pests (EPPO, 2022). In addition to ease of mechanical transmission, possibility to survive outside of the host on inert and biological surfaces, and long-distance dispersal through offshore seed production such as other tobamoviruses, ToBRFV is of special concern because of its ability to break resistance of the *Tm*-2/Tm-2^2 (and *Tm-1*) resistance genes, which are present in many commercial tomato cultivars (Zhang, Griffiths, Marchand, Bernards, & Wang, 2022). This virus infects up to 100% of the plants in a crop and can cause a loss 30–70% of the tomato yield, mainly due to the reduction of plant vigor and therefore the length of the harvesting period. Moreover, the symptomatic fruits of infected plants lose market value or are unmarketable (EPPO, 2022). Control measures applied to eradicate, contain, or limit the impact of ToBRFV in host crops are classical measures against tobamoviruses. These measures are limited to the disposal of infected plants, the use of ToBRFV free planting material and sanitation methods. Currently, disinfection systems are not very effective and often not completely safe for operators (EPPO, 2022).

In this study the antiviral activity of the methanolic extracts of the commercial cloves of the four garlic types was evaluated against ToBRFV by an *in vitro* experiment, followed by mechanical inoculation on test plants (Iobbi et al., 2022). The viral deactivation, as a possible consequence of disassembly of virus coat protein (CP), was showed by the absence of detectable RNA genome of ToBRFV, after a short exposure to the extracts, in combination with the absence of viral genome in the young leaves of the artificially infected host plant. In addition to other biological functions, *Tobamovirus* CP protects the single RNA strand in an ordered dimer structure of a bilayered cylindrical disk (Bhyravbhatla, Watowich, & Caspar, 1998). The interactions between CP chain A and chain B are mediated by residues that are located between the two subunits and they are considered essential in maintaining the three-dimensional structure to stabilize the virion and to prevent virus disassembly (Lu, Taraporewala, Stubbs, & Culver, 1998). Based on these considerations, docking studies were carried out to investigate the possible interaction of the identified sulfur compounds in the active site of the virus CP, with the residues involved in the disassembly of viral particles, by means of a previously defined homology model of ToBRFV CP (Iobbi et al., 2022).

2. Materials and methods

2.1. General experimental procedures

Ultra-pure water and all organic solvents of analytical grade were purchased from ROMIL-UpS™ (Waterbeach, Cambridge, UK). The standard compounds (98% purity) *S*-allyl-L-cysteine and (±)-L-alliin chosen as representative of their main class were purchased from Merck KGaA (Darmstadt, Germany).

2.2. Sample collection and preparation of the extracts

The garlic accessions were grown under identical agricultural management practices to avoid interference from the other factors. A total of 22 accessions of Vessalico garlic, 12 and 6 of the French cultivars Messidrôme and Messidor, respectively, and 12 of "Aglio di Caraglio" were collected and authenticated based on clove morphology (Table S1, Supporting Information). Each accession was harvested in the phase of full ripeness, as evidenced by neck falling or drying of leaves, and stored at cellar temperature. The study was done in late autumn, five months after harvest, to reproduce the same conditions as commercial garlic that is sold throughout the autumn and the following winter season. Randomly selected clove samples were collected. Individual cloves were skinned carefully and subjected to extraction. Garlic extracts were prepared following the method reported by Liaqat et al. (Liaqat, Zahoor, Atif Randhawa, & Shahid, 2019) with slight modifications. Briefly, 36 g of peeled and crushed cloves from each ecotype were mixed with 150 mL ethanol/H_2O 1:1. Mixtures were sonicated (VWR USC200TH, VWR International, Leuven, Belgium) at fixed frequency of 37 KHz for 5 min and placed in orbital shaker (300 rpm, 40 °C) for 2 h followed by sonication and shaking up to 6 h. Filtered extracts were evaporated using rotary evaporator and the resultant viscous fluids were freeze dried. The extract powders were then stored in capped glass vials in laboratory

freezer.

2.3. Phytochemical analysis

Firstly, a full scan method was set up on a high-resolution mass spectrometry (Q Exactive™ Plus Hybrid Quadrupole-Orbitrap™ Mass Spectrometer, Thermo Fisher Scientific Inc., Waltham, MA, USA) to characterize the specialized metabolites of garlic. LC-MS data were acquired in positive ion mode, the mass parameters were setup up as follows: capillary temperature sets at 320 °C, flow rate of sheath gas and auxiliary gas set at 35.0 and 15 arbitrary units with a spray voltage of 3 KV. The compound identification criteria were based on accurate mass value, MS^2 experiments and literature data. Comparative analysis of organosulfur were performed in multiple reaction monitoring (MRM) mode to obtain more accurate data using a triple quadrupole instrumentation. A Nexera X2 UPLC (Shimadzu, Kyoto, Japan) coupled with an AB Sciex API6500 Q-Trap (AB Sciex, Framingham, MA, USA) spectrometer was adopted. The analyses were performed in positive ion mode (Fig. S1, Supporting Information). The HPLC analyses were performed on a reverse phase C18 column (100 × 2.1 mm, 1.6 μm particle size, Luna Omega, Phenomenex, Torrance, CA, USA), using H_2O formic acid 0.1% as eluent A and MeOH as eluent B. The elution condition was a linear gradient from 3 to 8% of B in 5 min followed by a second gradient step until 27% of B in 12 min. The flow rate was 0.25 mL/min, and the injection volume was 10 μL. The MS parameters were setup for all analytes (Table S2, Supporting Information). The chromatographic data and ESI-MS data of compounds detected in the extracts are reported in Table S3 (Supporting Information). For each experimental point, three technical replicates were performed. The results (Table S4, Supporting Information) were expressed as average ± standard deviation, where for each metabolite the average represents the compound area over the internal standard (IS) of three independent replicates.

2.4. Multivariate analysis

Systat software for Windows Version 13 (Systat Software Inc., IL, USA) was used for classical statistical analysis. The correlations between the chemical variables, computed using the Pearson correlation coefficient, were visualized by HC (single linkage as agglomeration algorithm). Cluster analysis was also applied for detecting similarities among the samples (single linkage based on Euclidean distance). PCA was applied on the autoscaled data. ANOVA analysis was run on the scores of PCA. Statistical significance was set at $p < 0.05$. Matrix Laboratory (MATLAB) (MathWorks, Inc., MA, USA) software jointly with SOM toolbox 2.1 were also used.

2.5. Antiviral activity

The effectiveness of the garlic extracts in degrading the RNA of the viral agent ToBRFV on a contaminated surface was evaluated by *in vitro* test (repeated three times). The inoculum was collected in Sicily (Italy) in April 2020. A cotton swab dipped in 10.0 mL of COPAN SRK® (Copan Diagnostics, Inc. Murrieta, CA, USA) modified universal neutralizing solution (UNS) was used for the sample uptake. The swab solution and the cotton swab were analyzed immediately upon arrival in the laboratory (2 days after sampling), to confirm the presence of ToBRFV. A volume of 0.1 mL modified UNS infected with ToBRFV was used for the inoculation of the well's flat bottom surface in a multiwell plate (Greiner Bio-One GmbH, Frickenhausen, Germany). Based on previous results (Iobbi et al., 2022) and on the usual application rate of commercial active ingredients for disinfection in agricultural facilities (Li, Baysal-Gurel, Abdo, Miller, & Ling, 2015), three different concentrations of the extracts, namely 64 ppm, 32 ppm and 6.4 ppm, were tested in a preliminary assay. The test was carried out as previously reported (Iobbi et al., 2022). 64 ppm was the minimum concentration to RNA degradation (Table S5, Supporting Information), and was selected for the antiviral activity assay for all other accessions.

After each *in vitro* test, the swabs used in the treated wells and controls (not treated wells) were used to verify the viability of the pathogen. Three different healthy tomato plants at BBCH (Biologische Bundesanstalt Bundessortenamt Chemische Industrie) (Meier, 2018), scale growth stage 22, per swab were mechanically inoculated. The abrasive carborundum (Merck KGaA, Darmstadt, Germany) was added to the tubes (1 g for tubes containing 10 mL solution and 0.1 g for tubes containing 0.9 mL solution). The inoculation was performed by dipping the cotton swab in the tube and rubbing the upper surface of the leaves. Plants were maintained in a containment greenhouse for 5 weeks. A symptom observation was conducted to evaluate the symptoms expression at 10, 21, and 35 days after the inoculation.

The swabs used for the inoculations as well as the swabs used for the sampling of treated and untreated wells were checked by molecular analysis to verify the presence of ToBRFV. In addition, after the last observation made at 35 days after the plant inoculation, samples consisting of 6 leaves obtained from each group of 3 replicated plants (plants inoculated with the same swab) were analyzed for the presence of ToBRFV. Total RNA was extracted with RNeasy Plant Mini Kit (Qiagen GmbH, Hilden, Germany) from each swab solution, cotton swab and plant material following the manufacturer's instructions. RT-PCR (Retro Transcriptase-Polymerase Chain Reaction) was performed according to EPPO protocols (EPPO, 2021).

2.6. Molecular docking

The chemical structures of the organosulfur compounds were built with Maestro Build Panel (Schrödinger, 2021). Each ligand was then energetically minimized with Ligprep module (Schrödinger, 2021) using OPLS3e force considering all possible tautomers and protonation states at pH 6.0 ± 1.0.

The homology model of ToBRFV CP was developed in a previous work (Iobbi et al., 2022) on the TMV CP backbone (PDB code: 1ei7, no ligand bound) (Bhyravbhatla et al., 1998) using Maestro Version 12.6.144 Prime Homology Modeling (Schrödinger, 2021). A 35 Å grid box was set up at the active site of ToBRFV CP, between the two CP subunits, using Receptor Grid Generation tool in the Glide module (Schrödinger, 2021). This grid involved Asn73, Ala74, Val75, Lys134, Thr136, Gly137, Tyr139, Ser143, Lys253, Val255, Val260, and Lys268 residues according to the literature (Zhao et al., 2020).

Molecular docking was performed using both Glide-SP and Glide-XP flexible docking protocols in Glide module (Schrödinger, 2021) resulting in a similar energy matching and binding poses. To analyse the ligand interactions the Protein–ligand Interaction Profiler tool (Adasme et al., 2021) and Ligand interaction diagram Maestro's tool (Schrödinger, 2021) were used.

3. Results and discussion

3.1. Quali-quantitative profiles of organosulfur compounds

The agricultural practice of buying non-local garlic bulbs for planting is widespread. The morphological and organoleptic characteristics of the obtained bulbs can be unpredictable and may raise quality issues because of the high degree of variability due to the high adaptability of the species (Hirata, Abdelrahman, Yamauchi, & Shigyo, 2016). As organosulfur compounds have been reported as a tool to distinguish garlic ecotypes (Montaño, Beato, Mansilla, & Orgaz, 2011), a LC-MS profile of 52 garlic accessions comprising the Italian "Aglio di Vessalico" and "Aglio di Caraglio", and the two French cultivars (Messidrôme and Messidor) was performed. 19 sulfur compounds were detected (Table S2, Supporting Information), comprising the major flavour precursor in intact garlic *S*-alk(en)ylcysteine sulfoxides (SACOs) [*S*-allyl-cysteine sulfoxide (ACSO or alliin), *S*-methyl-cysteine sulfoxide (methiin)] (Block, Naganathan, Putman, & Zhao, 1992), and γ-glutamyl peptides such as

γ-glutamyl-*S*-methyl-cysteine (GSMC), γ-glutamyl-phenylalanine (GPA), and γ-glutamyl-*S*-alk(en)ylcysteines (GSAkCs) [γ-L-glutamyl-*S*-allyl-L-cysteine (GSAC), γ-glutamyl-*S*-(*trans*-1-propenyl)-cysteine (GS1PC)], the major polar sulfur compounds found in the homogenate of fresh-picked garlic (Lawson, Wang, & Hughes, 1991), intermediates in the metabolic pathway of alliin's biosynthesis, and considered also as the storage pools of nitrogen and sulfur within the cell (Martins et al., 2016). *S*-Allyl-glutathione (SAG) is thought to exist in raw garlic as an intermediate on alliin synthesis pathway (Kodera, Kurita, Nakamoto, & Matsutomo, 2020). Additionally, characteristic compounds of aged garlic were identified. *S*-Alk(en)ylcysteines [*S*-allyl-cysteine (SAC), *S*-methyl-cysteine (SMC)] are odourless and stable hydrophilic sulfur compounds produced by the catalytic activity of endogenous γ-glutamyl transpeptidase (GGT) that cleaves the γ-glutamyl group from γ-glutamyl-*S*-alk(en)ylcysteine sulfoxides during aging process (Kodera et al., 2020). *S*-1-Propenyl-L-cysteine (S1PC) is a stereoisomer of SAC. The amount of S1PC is less than the limit of detection in fresh garlic cloves. It has been identified in aged garlic extract, where it is formed by the same mechanism as SAC (Kodera, Ushijima, Amano, Suzuki, & Matsutomo, 2017). γ-Glutamyl-*S*-allyl-mercapto-cysteine (GSAMC) is obtained from γ-glutamyl-*S*-allylcysteine (GSAC)/γ-glutamyl-*S*-1-propenylcysteine (GS1PC) during the early stage of the aging process (Fujii, Matsutomo, &

Table 1
LC-MS analyses of organosulfur compounds for each of the four garlic types.

Name of the analyte (ID)	Vessalico	Caraglio	Messidor	Messidrôme
S-methyl-cysteine sulfoxide (methiin)	15.02 ± 17.82; 8.96; 0.47–64.15	0.74 ± 0.43; 0.91; 0.05–1.22	8.63 ± 6.25; 12.51; 0.51–12.95	20.80 ± 9.59; 22.06; 8.52–36.01
S-allyl-L-cysteine sulfoxide (alliin)	139.20 ± 103.96; 80.16; 21.10–382.78	6.16 ± 4.57; 8.93; n.d.–9.76	75.47 ± 58.61; 109.59; n.d.–118.26	100.23 ± 49.60; 105.50; 38.18–185.88
S-methyl-cysteine (SMC)	12.88 ± 7.96; 12.65; 2.14–28.07	12.49 ± 4.47; 11.28; 5.78–20.20	8.08 ± 1.91; 7.59; 6.11–10.50	14.22 ± 4.17; 13.95; 8.33–20.33
S-allyl-cysteine (SAC)	112.11 ± 48.55; 104.29; 29.34–205.58	53.50 ± 20.76; 50.61; 24.27–88.50	96.22 ± 22.77; 90.61; 64.76–124.60	350.89 ± 108.31; 357.17; 194.53–561.85
γ-glutamyl-*S*-methyl-cysteine (GSMC)	42.75 ± 32.60 29.58 11.63–129.28	32.44 ± 8.26 30.33 19.58–46.24	19.57 ± 7.55 18.11 12.12–32.57	84.81 ± 27.54 77.20 56.18–150.29
fructosyl-*S*-allyl-cysteine (Fru-SAC)	5.49 ± 2.85 4.78 1.47–11.12	3.20 ± 2.09 2.21 1.11–7.38	6.08 ± 1.90 5.65 3.85–8.99	19.75 ± 6.30 21.10 8.78–30.37
fructosyl-*S*-(*trans*-1-propenyl)-cysteine (Fru-S1PC)	5.55 ± 3.58 5.45 0.40–14.33	3.85 ± 2.16 3.02 1.63–8.22	9.59 ± 1.70 9.76 7.57–12.34	21.01 ± 7.12 19.57 9.45–36.07
S-allyl-mercapto-cysteine (SAMC)	19.59 ± 9.63 19.46 2.15–37.70	3.08 ± 1.99 3.46 0.27–6.17	9.89 ± 6.94 11.93 1.23–18.12	31.27 ± 13.61 35.15 12.37–53.10
γ-glutamyl-γ-glutamyl-*S*-methyl-cysteine (GGSMC)	12.14 ± 10.33 9.48 2.28–39.40	3.18 ± 0.74 3.17 1.90–4.30	6.04 ± 1.78 6.10 3.66–8.31	24.73 ± 7.11 22.27 18.43–39.71
S-allyl-glutatione (SAG)	2.35 ± 2.57 0.94 0.49–10.14	1.93 ± 0.85 2.26 0.68–3.08	1.26 ± 1.15 0.73 0.32–3.05	0.90 ± 0.31 0.86 0.54–1.64
γ-glutamyl-*S*-allyl-cysteine (GSAC)	757.55 ± 318.71 672.37 334.59–1549.48	356.05 ± 94.68 331.54 211.71–534.19	354.39 ± 76.11 351.46 273.76–456.89	1091.71 ± 362.15 1103.32 701.26–1925.87
fructosyl-γ-glutamyl-*S*-allyl-cysteine (Fru-GSAC)	11.15 ± 5.01 10.42 5.04–27.20	6.99 ± 2.82 6.77 2.71–11.52	7.93 ± 3.48 7.24 3.81–12.91	22.22 ± 13.42 14.50 8.68–46.16
γ-glutamyl-*S*-(*trans*-1-propenyl)-cysteine (GS1PC)	318.67 ± 203.50 252.18 133.41–903.72	181.07 ± 40.37 181.26 120.04–268.10	209.31 ± 39.87 208.40 155.97–268.11	417.03 ± 117.65 374.41 299.64–696.60
γ-glutamyl-γ-glutamyl-*S*-allyl-cysteine (GGSAC)	5.56 ± 2.70 6.13 1.12–9.25	2.73 ± 0.75 2.75 1.67–3.87	3.41 ± 0.82 3.51 2.48–4.56	29.56 ± 6.00 27.58 23.78–42.13
fructosyl-γ-glutamyl-*S*-(*trans*-1-propenyl)-cysteine (Fru-GS1PC)	6.51 ± 3.47 5.79 2.44–15.27	5.24 ± 2.16 5.24 2.08–9.41	7.85 ± 4.06 7.51 2.87–13.68	12.18 ± 8.28 7.23 4.79–28.49
γ-glutamyl-phenylalanine (GPA)	180.42 ± 55.05 174.14 107.44–316.89	348.24 ± 88.51 320.67 215.76–519.45	93.72 ± 7.95 94.81 83.70–104.34	302.78 ± 62.63 299.29 208.70–438.41
γ-glutamyl-γ-glutamyl-*S*-(*trans*-1-propenyl)-cysteine (GGS1PC)	4.98 ± 2.97 3.49 0.91–9.60	3.42 ± 0.73 3.49 2.06–4.49	5.50 ± 0.91 5.79 4.26–6.38	26.56 ± 6.12 24.87 19.77–39.27
S-allyl-mercapto-glutatione (SAMG)	0.91 ± 0.76 0.65 0.23–2.90	0.28 ± 0.23 0.22 0.05–0.65	0.25 ± 0.13 0.25 0.09–0.44	0.06 ± 0.01 0.06 0.04–0.09
γ-glutamyl-*S*-allyl-mercapto-cysteine (GSAMC)	43.99 ± 16.54 45.08 19.48–81.45	21.07 ± 6.93 21.48 12.03–30.67	21.84 ± 3.45 22.76 17.51–25.82	89.13 ± 16.48 84.25 70.39–123.50

Data are expressed as mean of averages (average represents the relative content expressed as areas over the internal standard, IS) ± standard deviation; median; range.

Kodera, 2018). *S*-Allyl-mercapto-cysteine (SAMC) is not detected in fresh whole garlic, and only a trace amount is found when garlic is crushed (Kodera et al., 2020). SAMC is produced from GSAMC by GGT (Fujii et al., 2018) and *S*-allyl-mercapto-glutathione (SAMG) is produced by reaction of allicin with glutathione (Rabinkov et al., 2000). The γ-glutamyl-γ-glutamyl-*S*-alk(en)ylcysteine derivatives [γ-glutamyl-γ-glutamyl-*S*-methyl-cysteine (GGSMC), γ-glutamyl-γ-glutamyl-*S*-allyl-cysteine (GGSAC), γ-glutamyl-γ-glutamyl-*S*-(*trans*-1-propenyl)-cysteine (GGS1PC)] are present only in traces in raw garlic. The 80% of the content of these γ-glutamyl tripeptides is produced from γ-glutamyl dipeptides by the endogenous GGT within 1 month during the aging process, reaches the maximum levels after approximately 4 months of aging, and gradually decreases during the subsequent aging process (Nakamoto, Fujii, Matsutomo, & Kodera, 2018). Finally, the Heyns compounds (Yuan, Sun, Chen, & Wang, 2016) fructosyl-*S*-allyl-cysteine (Fru-SAC), fructosyl-*S*-(*trans*-1-propenyl)-cysteine (Fru-S1PC), fructosyl-γ-glutamyl-*S*-allyl-cysteine (Fru-GSAC), and fructosyl-γ-glutamyl-*S*-(*trans*-1-propenyl)-cysteine (Fru-GS1PC) were detected. These compounds are present at very low amounts in fresh raw garlic and are produced by the Maillard reaction during the aging process from GSAC and GS1PC (Kodera et al., 2020).

Table 1 reports the relative content of the 19 sulfur compounds detected for each of the four garlic types. The presence and the relative content of the compounds were in agreement with the aging and storage conditions of the garlic accessions (Beato, Sánchez, de Castro, & Montaño, 2012). A wide range of variation was observed, from the maximum of GSAC to the minimum of SAMG, 100-fold less abundant for all the types. The relative content of GS1PC, GPA, and SAC were high for all the types, while SAG was low. Vessalico, Messidor and Messidrôme showed a remarkable relative content of alliin, higher than most of the other compounds and literature data (Diretto et al., 2017). This could be related to the usual storage of commercial garlic bulbs at cellar temperature for six-eight months after harvest, to ensure year-round supply for customers (Ichikawa, Ide, & Ono, 2006). In these storage conditions, γ-glutamyl peptides can be converted into sulfoxides (Hornickova et al., 2010). Moreover, all the garlic types showed relative levels of SMC and SAC from 100- to 1000-fold higher than literature data (Diretto et al., 2017), because of aging process.

As shown in Table 1, a different data dispersion was observed within each of the four garlic types, generally larger for Vessalico accessions. Moreover, differences between mean and median values were found for some compounds, thus indicating skewed distributions. Some outliers for methiin, alliin, GSMC, SAG, GS1PC and SAMG among the Vessalico accessions, and some for Fru-GSAC e Fru-GS1PC among the Messidrôme were detected.

3.2. Multivariate analysis

To investigate the relationships among the relative content of the 19 sulfur compounds in the extracts, correlation analysis was performed, showing that several of the measured variables were significantly correlated (Table S6, Supporting Information). The results, visualized in form of similarity dendrogram as obtained by HC, are reported in Fig. 1a. Most sulfur compounds were agglomerated in a large cluster, where the most correlated variables were GGSAC, GGS1PC and SAC. All these compounds were from 3- to 10-fold abundant in Messidrôme. GGSMC and GS1PC were also strongly correlated and abundant in Messidrôme and in some Vessalico accessions. The fructosyl compounds were abundant in Messidrôme. The highest correlations were between Fru-SAC and Fru-S1PC, and between Fru-GSAC and Fru-GS1PC at lesser extent. A different behavior was shown by SMC and GPA, not correlated with any other variable. SAG was only correlated with SAMG, due to the strong leverage effect of four Vessalico accessions (A9, A21, A35, A47) with anomalous high content compared with the other samples.

HC applied to garlic accessions (Fig. S2, Supporting Information) showed Caraglio as a compact group. Vessalico, except for a small number of accessions, was joined with Messidor. Two clusters of Messidrôme were detected.

The results of HC were confirmed by PCA. The biplot of the 52 accessions described by the 19 sulfur compounds on the plane of the first two principal components (PCs) is shown in Fig. 1b. The 15 compounds forming the large cluster in Fig. 1a showed high loadings on PC1, and clearly separated Messidrôme accessions at high content of these variables. Alliin, SAMG and SAG had high loadings on PC2: on this axis some Vessalico accessions (A4, A9, A30, A35) at high content of alliin, SAG, SAMG, and low content of SMC, Fru-SAC and Fru-S1PC were evident (Fig. 1b). Caraglio garlic appeared as a more compact group, not overlapping with the other types, while Vessalico appeared as a disperse group, overlapping with Messidor accessions. This result is consistent with the fact that the growers of the area of Vessalico purchase cloves of Messidor and Messidrôme cultivars every year in France for sowing, while Caraglio farmers use the cloves of own production. The biplot of the samples and variables on the plane of PC3 and PC4 is shown in Fig. S3 (Supporting Information). Fru-GSPC, Fru-GSAC and SMC showed high loadings on PC3; GPA and SAMG were the only variables contributing to PC4. Two groups of Messidrôme accessions were detected; one of them (A7, A25, A33, A51) was very close to two Vessalico samples (A20 and A46), well separated on PC3, at high content of Fru-GS1PC, Fru-GSAC and low content of SMC. Caraglio accessions at high content of GPA resulted well separated on PC4, together with two Vessalico (A4 and A30); on the same axis, some other anomalous Vessalico accessions

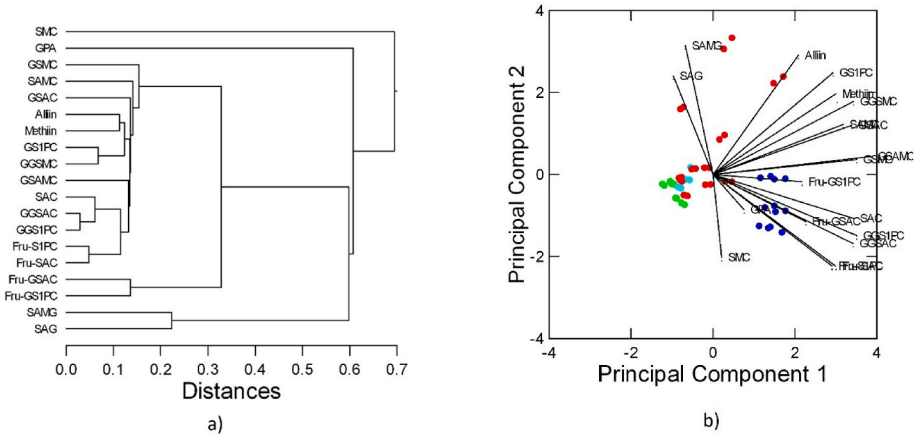

Fig. 1. Results of multivariate analysis (HC and PCA). a) Similarity dendrogram obtained from cluster analysis (single linkage method based on Pearson coefficients) applied to the 19 sulfur compounds determined by LC-MS analyses on 52 garlic accessions; b) Biplot showing the scores of the 52 samples (● = Vessalico; ● = Caraglio; ● = Messidor; ● = Messidrôme) and the loadings of the 19 variables on Principal Components 1 and 2 (respectively, 48% and 21% of the total variance).

(A9, A21, A35, A47) showed high content of SAG and SAMG.

The scores of PCA were submitted to ANOVA analysis to test the possibility of discriminating between samples belonging to the four types: significant differences ($p < 0.0005$) were found for PC1, PC2 and PC4. A post-hoc test (Tukey test) found a significant difference between the samples of Messidrôme and the other three classes ($p < 0.0005$) when the scores on PC1 were considered; Vessalico garlic was significantly different from Messidrôme ($p < 0.0005$) and Caraglio ($p < 0.01$) when the scores on PC2 were considered, while Caraglio was significantly different ($p < 0.01$) from the others on the basis of the scores on PC4 (Fig. S4, Supporting Information).

Finally, data analysis was performed by SOM. To prevent higher range variables to dominate the map due to their greater impact on the involved distances, the data were normalized before submitting them to the algorithm. Specifically, a variance-based normalization was performed. Subsequently, linear initialization and batch training were carried out. The training was carried out in two phases: initially the coarser phase with a larger radius and learning rate - a parameter that determines the step size at each iteration while moving toward a minimum - that also considers more distant nodes and a refinement phase with a smaller radius and learning rate. After these steps, the U-matrix (unified distance matrix) was generated (Fig. 2, at the top left). It is a visual representation of a SOM and displays the distances between neighbouring map units (neurons) and can therefore display the structure of the clusters in the map. Higher values indicate a cluster edge, while uniform areas identify clusters. In the component plan (Fig. 2, other maps), those that are similar to each other identify highly correlated variables. Specifically, we can confirm as an example the strict correlation between GGSAC and GGS1PC and between Fru-GSAC and Fru-GS1PC, with the two couples significantly different with each other. Fig. 3a shows a similarity colouring, made by spreading a colormap on top of the PC projection of the prototype vectors. Similarities between samples are identified by associating a similar colour code for samples with similar characteristics, together with clustering information and the number of hits in each unit. Hits are the number of times for which a single map unit responds to inputs and indicate how the number of input information are collected in each neuron. Labels for the hits are shown in Fig. 3b. The choice of the number of neurons is correct with respect to the number of samples since the entire surface of the map is used and there is no overlap between samples. Neurons containing the Vessalico type hold the central and top left parts of the map, and they were well separated from other types. A neuron containing four Vessalico (A12, A23, A38, A49) accessions in the right centre of the map was the only exception. A Messidor neuron was bordering with the Vessalico neuron, indicating their greater similarity. No Caraglio neurons were close to the Vessalico ones.

From a more quantitative point of view, the map data were analyzed using the k-means algorithm, which provides a division of the map values into k clusters. The obtained clusters were validated with the Davies-Bouldin index (DBI) (Davies & Bouldin, 1979), identifying 6 as the number of optimal clusters, corresponding to the minimum value obtained from the DBI (Fig. 3c). Cluster analysis identified three sub-classes in Vessalico type, namely I (A20, A21, A46, A47), II (A4, A9, A30, A35), and III (A1, A6, A13, A18, A22, A27, A32, A39, A44, A48), attributable to three different areas of the territory of Vessalico. All the accessions came indifferently by cloves of Messidor and Messidrôme. The fact that these accessions had different genotype but were cultivated in the same geographical location and with the same agricultural practice could indicate as conditions of growth, harvest and post-harvest may be more important than the original genotype for the composition of garlic clove sulfur compounds (Martins et al., 2016; Montaño et al., 2011), and could lead to define Vessalico garlic as an agricultural ecotype.

3.3. Antiviral activity assay and evaluation of final viability of the virus

In vitro tests in a multiwell plate, in combination with plant inoculation, were performed to evaluate the antiviral activity of the garlic extracts. Briefly, after a short exposure to the treatments, the presence of detectable genome of ToBRFV in the inoculated and treated wells was verified by molecular detection of different encoding regions of the virus. Afterwards, a biological assay was carried out to check that the

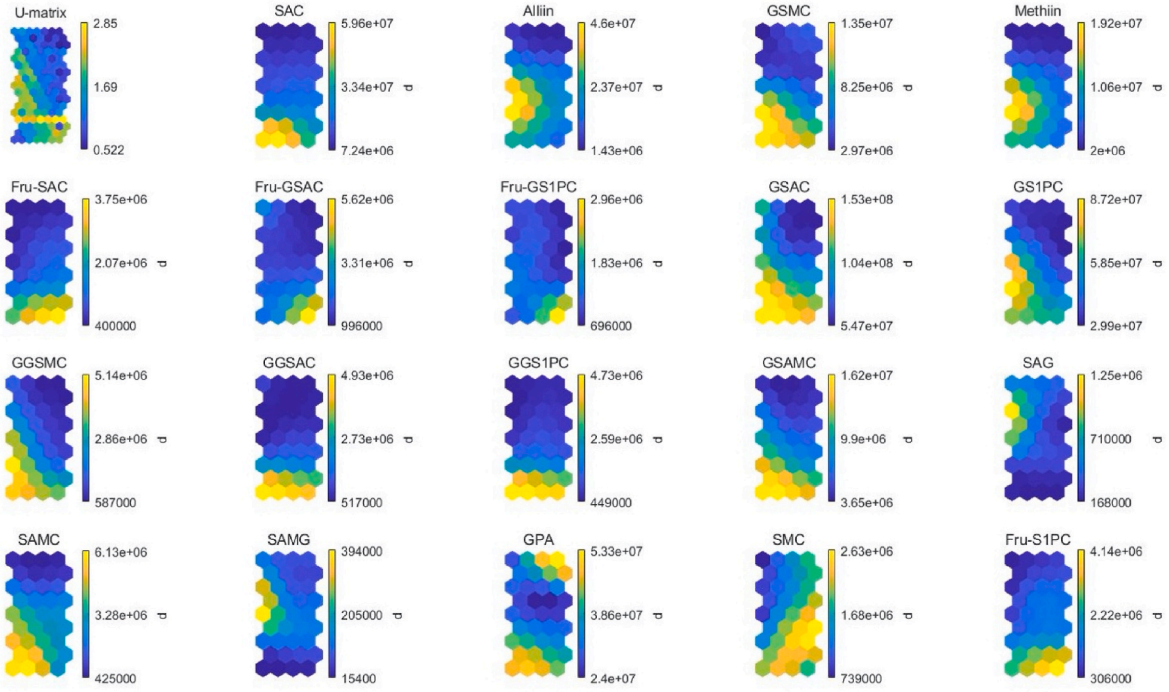

Fig. 2. SOM, U-matrix and maps for each organosulfur compound. Similar colour gradations indicate highly correlated variables. (For interpretation of the references to colour in this figure legend, the reader is referred to the Web version of this article.)

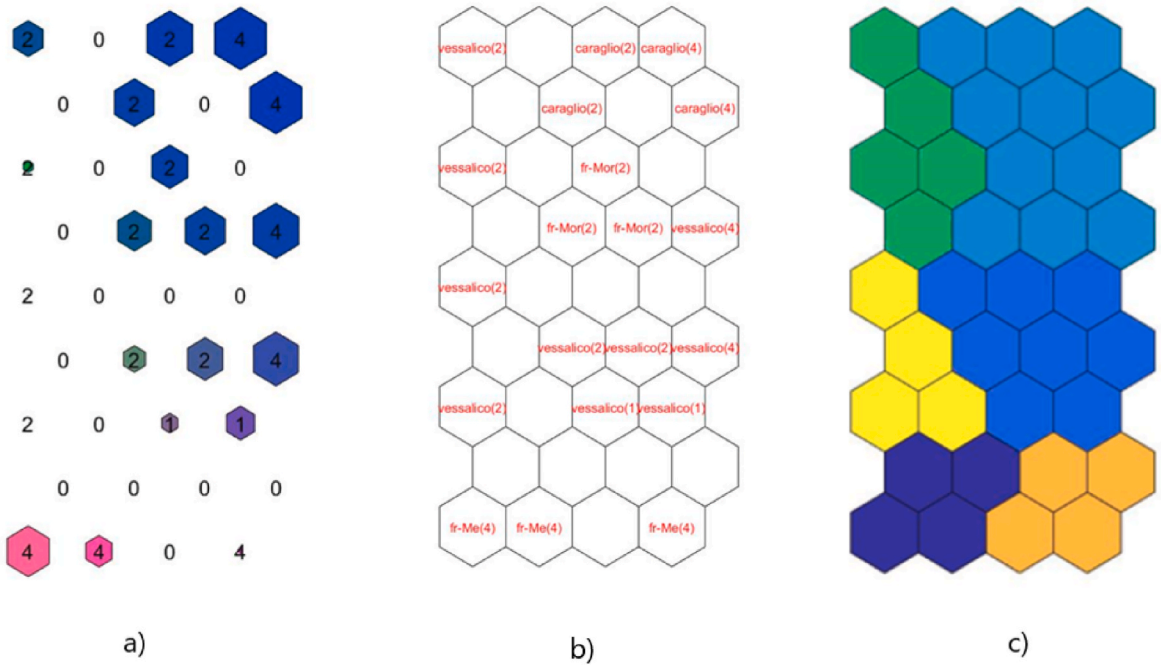

Fig. 3. Graphical representation of map. a) SOM output map with colour code association. Similar colours have similar characteristics, numbers correspond to hit numbers. Dimensions of hexagons are related to the distance between neurons (biggest indicates greater distance); b) Labelled SOM output map, for each neuron the corresponding classes are shown (fr-Mor = Messidor; fr-Me = Messidrôme); c) Clustering of the map (colours are arbitrary). (For interpretation of the references to colour in this figure legend, the reader is referred to the Web version of this article.)

Table 2
Docking interaction parameters of the sulfur compounds.

Ligand acronym	Ligand name	Glide binding energy (kcal/mol)	H-bond interacting amino acids	Hydrophobic interactions/ π-cation interactions	Salt bridge
Fru-GSAC	fructosyl-γ-glutamyl-*S*-allyl-cysteine	−52.65	Glu131, Asp219, Glu222, Lys268	Ala74, Val75, Thr136, Pro254, Val255	Lys253, Lys268
Fru-GS1PC	fructosyl-γ-glutamyl-*S*-(*trans*-1-propenyl)-cysteine	−50.92	Asn73, Val130, Glu131, Lys134, Gly137, Asp219, Lys268	Lys134, Thr136, Val255, Val260	Lys268
GGS1PC	γ-glutamyl-γ-glutamyl-*S*-(*trans*-1-propenyl)-cysteine	−49.49	Asn73, Glu131, Gly137, Ser143, Asp219, Glu222, Lys253, Pro254, Lys268	Ala147, Val255, Val260	Lys253, Lys268
GGSAC	γ-glutamyl-γ-glutamyl-*S*-allyl-cysteine	−48.16	Asn73, Glu131, Ser143, Asp219, Glu222, Lys253, Lys268	Thr136, Ala147	Lys253, Lys268
GGSMC	γ-glutamyl-γ-glutamyl-*S*-methyl-cysteine	−44.23	Asn73, Glu131, Gly137, Tyr139, Asp219, Glu222, Lys253, Lys268	–	Lys253, Lys268
SAG	*S*-allyl-glutatione	−43.27	Asn73, Glu131, Glu222, Lys268	Lys134, Thr136, Asp219, Lys253	–
SAMG	*S*-allyl-mercapto-glutatione	−42.81	Glu222, Ser265, Gly266, Ly268	Val75	–
Fru-SAC	fructosyl-*S*-allyl-cysteine	−39.09	Val130, Glu131, Asp219, Glu222	Val75, Val255	Lys253, Lys268
Fru-S1PC	fructosyl-*S*-(*trans*-1-propenyl)-cysteine	−38.48	Val130, Lys134, Asp219, Glu222, Lys268	–	Lys134, Lys268
GSAMC	γ-glutamyl-*S*-allyl-mercapto-cysteine	−36.90	Glu131, Lys134, Asp219, Lys268	Val75, Lys134, Asp219	Lys268
	ribavirin[a]	−35.29	Asn73, Lys134, Gly137,		
GSAC	γ-L-glutamyl-*S*-allyl-L-cysteine	−34.01	Glu131, Glu222, Lys268	Lys134, Thr136, Asp219, Lys253	Lys268
GS1PC	γ-glutamyl-*S*-(*trans*-1-propenyl)-cysteine	−33.91	Asn73, Glu131, Gly137, Asp219	Val75, Thr136, Val255	Lys253, Lys268
GPA	γ-glutamyl-phenylalanine	−33.24	Asn73, Glu131, Gly137, Asp219, Glu222, Lys253, Lys268	Thr136, Val255, Val260, Pro263	Lys253, Lys268
GSMC	γ-glutamyl-*S*-methyl-cysteine	−32.89	Glu131, Asp219, Glu222, Lys253, Lys268	Thr136, Val255	Lys253, Lys268
alliin	*S*-allyl-cysteine sulfoxide	−23.06	Glu131, Lys134, Lys268	Val255	Glu131
SAMC	*S*-allyl-mercapto-cysteine	−24.08	Asn73, Gly137, Val255	Thr136, Lys253, Val255	–
methiin	*S*-methyl-cysteine sulfoxide	−23.11	Glu131, Lys268	–	Glu131, Lys268
SAC	*S*-allyl-cysteine	−20.99	Lys134, Lys268	–	Glu131, Lys268
SMC	*S*-methyl-cysteine	−18.44	Glu131, Lys268	–	Lys268

[a] Ribavirin, a *Tobamovirus* inhibitor, was used as a reference ligand (Iobbi et al., 2022).

pathogen was no longer viable.

Results obtained by the molecular detection of ToBRFV are summarized in Table S7 (Supporting Information). Swabs used for the sampling of inoculated and treated wells, as well as negative control swabs, were negative for the presence of the virus, unlike positive control swabs. Immediately after the antiviral activity assay, mechanical inoculation (treated and not treated) of healthy plants was done to verify the final viability of the virus. Results obtained by the molecular detection of ToBRFV 35 days after the inoculation are reported in Table S8 (Supporting Information). 21 days after the inoculation, positive control plants developed symptoms (blistering, distortion, and narrowing of leaves) in all the three experiments. Molecular analysis performed on the new apical leaves 35 days after the inoculation gave positive result for the presence of the virus. Plants inoculated with swabs used for the sampling of inoculated and treated wells, as well as negative control plants, did not develop symptoms. Molecular analysis was negative for the presence of the virus in all three experiments for all the accessions.

3.4. Molecular docking

Molecular docking studies were carried out to investigate the possible interaction between the organosulfur compounds and ToBRFV CP. In computational simulations all ligands were positioned as inhibitors between the two subunits of CP that protect the single strand RNA. All the sulfur compounds directly interacted with important residues in the ToBRFV CP active site, thus preventing the assembly of the CP and blocking the interactions between viral CPs involved in the infection (Zhao et al., 2020). Ribavirin, a *Tobamovirus* inhibitor, was used as a reference ligand (Iobbi et al., 2022). Ligand-binding energies and interactions are listed in Table 2. Most of the compounds showed higher binding energy than ribavirin. In a previous work (Iobbi et al., 2022), ribavirin showed a binding energy value of −35.29 kcal/mol, and it displayed five H-bonds formed by the β-D-ribofuranosyl moiety in the protein active site. The hydroxyl groups and the carboxamide group of ribavirin emerged as essential to prevent interaction between the two CP subunits. In this study, Fru-GSAC achieved the best binding energy value (−52.65 kcal/mol) followed by Fru-GS1PC, GGS1PC, GGSAC, and GGSMC. Fru-GSAC emerged as strongly bound to ToBRFV CP by several residues located between the two CP-CP subunits. Fru-GSAC interacted with Ala74, Val75, Thr136, Pro254 and Val255 through hydrophobic interactions. The ligand was also involved in eight H-bonds with Glu131, Asp219, Glu222 and Lys268 (Figs. 4 and 1a,b). Fru-GS1PC displayed nine H-bonds in its binding with the target, with residues Asn73, Val130, Glu131, Lys134, Gly137 and Asp219 respectively. Lys134, Thr136, Val 255 and Val260 were also involved in hydrophobic interactions (Figs. 4 and 2a,b). The fructosyl moiety, structurally similar to the ribavirin's β-D-ribofuranosyl portion, particularly contributed to these interactions. GGS1PC, GGSAC and GGSMC reported comparable binding energy values and interactions in the ToBRFV CP active site, reasonably due to their similar scaffold. These complexes were further stabilized by salt bridges between their carboxylic group and Lys253 and Lys268 residues. Methiin and alliin showed a salt bridge with Glu131, and Fru-S1PC with Lys134. SAG and SAMG showed comparable binding energy values, −43.27 kcal/mol and −42.81 kcal/mol respectively. SAMG displayed a different pose probably due to the steric hindrance of the two sulfur atoms in the side chain. Glutathione moiety created a good interaction pattern as the glutamyl and the fructosyl moieties that allowed these compounds to strongly interact with the active site. Fru-SAC and Fru-S1PC displayed the same interactions at the active site, again depending on their similar scaffold. The binding results obtained for these two compounds highlight the glutamyl moiety as an important molecular feature for getting a high inhibitory potency on the target. Interaction and binding pose of other sulfur compounds in addition to Fru-GSAC and Fru-GS1PC are reported in Fig. S6 (Supporting Information).

4. Conclusions

Vessalico garlic type showed intermediate characteristics between the two parent cultivars, and the importance of the culture geographical location, as well as the agricultural conditions was underlined, allowing to define this garlic as an agricultural ecotype. All garlic accessions showed antiviral activity against ToBRFV. This is probably due to the synergistic effect of the various components of the extract (Rouf et al., 2020), even if molecular docking simulations showed that the Heyns

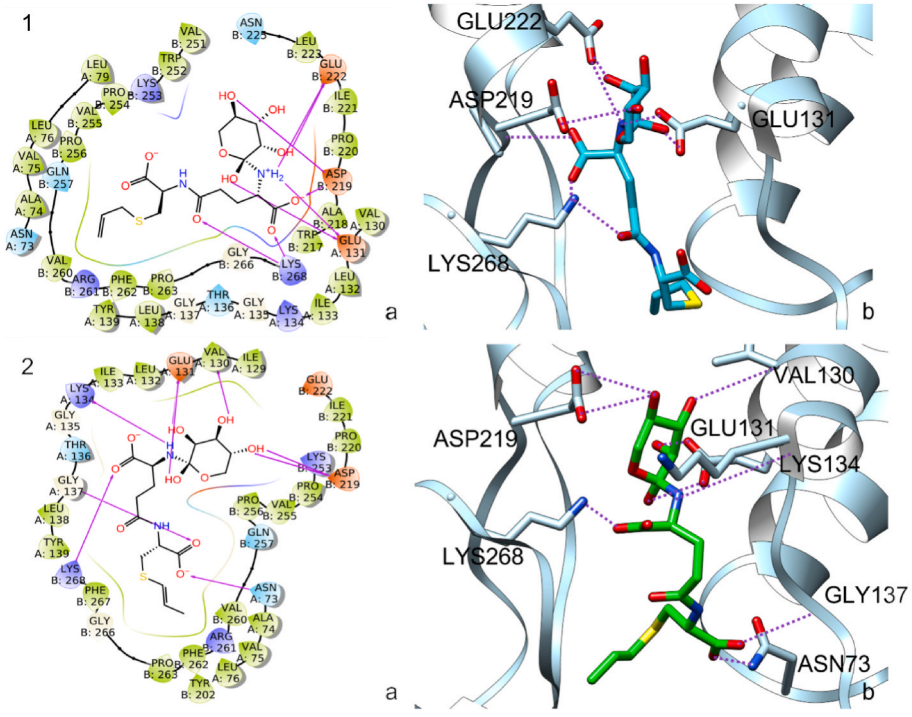

Fig. 4. Interaction (a) and binding pose (b) of fructosyl-γ-glutamyl-S-allyl-cysteine (Fru-GSAC) (1), and fructosyl-γ-glutamyl-S-(*trans*-1-propenyl)-cysteine (Fru-GS1PC) (2) at the ToBRFV CP active site. a) The ligands are surrounded by the protein residues represented as follows: the negatively charged residues are indicated in red, polar residues are in cyan, hydrophobic residues are shown in green; H-bonds are depicted as purple arrows; b) The protein is reported as light-blue ribbons; Fru-GSAC (1) is reported as cyan capped sticks; Fru-GS1PC (2) is reported as green capped sticks. H-bonds are presented as purple dotted lines. (For interpretation of the references to colour in this figure legend, the reader is referred to the Web version of this article.)

compounds produced by the Maillard reaction during the aging process and the γ-glutamyl-γ-glutamyl-*S*-alk(en)ylcysteine derivatives could be the main compounds responsible of the antiviral activity. Anyway, the antiviral activity seems to be more traceable to commercial garlic after several months from harvest. This result might be a good starting point for the possible use of garlic extracts as antiviral agent in organic agriculture, as recovery of waste product or unsold at the season end.

Declaration of competing interest

Declarations of interest: none.

Funding

This work was supported by EU INTERREG V ALCOTRA (2014–2020); PITER Project "ALPIMED INNOV" [grant number 4073].

CRediT authorship contribution statement

Valeria Iobbi: Methodology, Validation, Formal analysis, Investigation, Data curation, Writing – original draft. **Valentina Santoro:** Investigation, Formal analysis. **Norbert Maggi:** Software, Formal analysis. **Mauro Giacomini:** Methodology, Software, Formal analysis. **Anna Paola Lanteri:** Investigation, Data curation, Writing – original draft. **Giovanni Minuto:** Supervision. **Andrea Minuto:** Investigation. **Paola Fossa:** Validation. **Nunziatina De Tommasi:** Conceptualization, Writing – review & editing, Supervision. **Angela Bisio:** Conceptualization, Resources, Writing – review & editing, Supervision, Project administration, Funding acquisition. **Giuliana Drava:** Methodology, Validation, Formal analysis, Writing – review & editing.

Data availability

No data was used for the research described in the article.

Acknowledgements

The authors would like to thank "Centro di Sperimentazione ed Assistenza Agricola (CERSAA)", Albenga (SV), Italy, for coordinating the harvest of garlic samples, and the local farmers who supplied them.

Appendix A. Supplementary data

Supplementary data to this article can be found online at https://doi.org/10.1016/j.lwt.2022.114411.

References

Adasme, M. F., Linnemann, K. L., Bolz, S. N., Kaiser, F., Salentin, S., Haupt, V. J., et al. (2021). Plip 2021: Expanding the scope of the protein–ligand interaction profiler to DNA and RNA. *Nucleic Acids Research, 49*(W1), W530–W534. https://doi.org/10.1093/nar/gkab294

Beato, V. M., Sánchez, A. H., de Castro, A., & Montaño, A. (2012). Effect of processing and storage time on the contents of organosulfur compounds in pickled blanched garlic. *Journal of Agricultural and Food Chemistry, 60*(13), 3485–3491. https://doi.org/10.1021/jf3002075

Benke, A. P., Krishna, R., Mahajan, V., Ansari, W. A., Gupta, A. J., Khar, A., et al. (2021). Genetic diversity of Indian garlic core germplasm using agro-biochemical traits and SRAP markers. *Saudi Journal of Biological Sciences, 28*(8), 4833–4844. https://doi.org/10.1016/j.sjbs.2021.05.013

Bhyan, S. B., Alam, M. M., & Ali, M. S. (2007). Effect of plant extracts on *Okra mosaic virus* incidence and yield related parameters of *Okra*. *Asian Journal of Agricultural Research, 1*(3), 112–118. https://doi.org/10.3923/ajar.2007.112.118

Bhyravbhatla, B., Watowich, S. J., & Caspar, D. L. (1998). Refined atomic model of the four-layer aggregate of the *Tobacco mosaic virus* coat protein at 2.4-A resolution. *Biophysical Journal, 74*(1), 604–615. https://doi.org/10.1016/s0006-3495(98)77819-1

Block, E. (2010). *Garlic and other alliums - the lore and the science*. Cambridge, UK: The Royal Society of Chemistry.

Block, E., Naganathan, S., Putman, D., & Zhao, S. H. (1992). *Allium* chemistry: HPLC analysis of thiosulfinates from onion, garlic, wild garlic (ramsoms), leek, scallion, shallot, elephant (great-headed) garlic, chive, and Chinese chive. Uniquely high allyl to methyl ratios in some garlic samples. *Journal of Agricultural and Food Chemistry, 40*(12), 2418–2430. https://doi.org/10.1021/jf00024a017

Communication from the Commission to the European Parliament. (2020). *The council, the European economic and social committee and the committee of the regions. A farm to fork strategy for a fair, healthy and environmentally-friendly food system*.

Davies, D. L., & Bouldin, D. W. (1979). A cluster separation measure. *IEEE Transactions on Pattern Analysis and Machine Intelligence, 1*(2), 224–227. https://doi.org/10.1109/TPAMI.1979.4766909

Diretto, G., Rubio-Moraga, A., Argandoña, J., Castillo, P., Gómez-Gómez, L., & Ahrazem, O. (2017). Tissue-specific accumulation of sulfur compounds and saponins in different parts of garlic cloves from purple and white ecotypes. *Molecules, 22*(8). https://doi.org/10.3390/molecules22081359

EPPO. (2021). PM 7/146 (1) *Tomato brown rugose fruit virus*. *EPPO Bulletin, 51*(1), 178–197. https://doi.org/10.1111/epp.12723

EPPO. (2022). EPPO datasheet: Tomato brown rugose fruit virus. In European and mediterranean plant protection organization. EPPO. In *EPPO datasheets on pests recommended for regulation* (Paris, France).

European Parliament. (2009). Directive 2009/128/EC of the European Parliament and of the Council of 21 October 2009 establishing a framework for Community action to achieve the sustainable use of pesticides. *Official Journal of the European Union, Pub. L.* No. COD 2006/0132, EEA relevance 71-84 (2009 24.11).

Eurostat. Crop production in national humidity. Crop production (apro_cp) Reference Metadata in Euro SDMX Metadata Structure (ESMS). https://appsso.eurostat.ec.europa.eu/nui/submitViewTableAction.do.

Fujii, T., Matsutomo, T., & Kodera, Y. (2018). Changes of *S*-allylmercaptocysteine and γ-glutamyl-*S*-allylmercaptocysteine contents and their putative production mechanisms in garlic extract during the aging process. *Journal of Agricultural and Food Chemistry, 66*(40), 10506–10512. https://doi.org/10.1021/acs.jafc.8b02541

CTPS 1011290 - MESSIDOR GEVES. (2015a). Institut National de la Recherche Agronomique. In *Le catalogue officiel des espèces et variétés de plantes cultivées en France. 49071 Beaucouzé cedex, France: Groupe d'Etude et de contrôle des Variétés Et des Semences*.

Le catalogue officiel des espèces et variétés de plantes cultivées en France GEVES. (2015b). Institut National de la Recherche Agronomique. In *49071 Beaucouzé cedex, France: Groupe d'Etudes et de Contrôle des Variétés Et des Semences*.

Godlewska, K., Ronga, D., & Michalak, I. (2021). Plant extracts - importance in sustainable agriculture. *Italian Journal of Agronomy, 16*(2), 1851.

González, R. E., Soto, V. C., Sance, M. M., Camargo, A. B., & Galmarini, C. R. (2009). Variability of solids, organosulfur compounds, pungency and health-enhancing traits in garlic (*Allium sativum* L.) cultivars belonging to different ecophysiological groups. *Journal of Agricultural and Food Chemistry, 57*(21), 10282–10288. https://doi.org/10.1021/jf9018189

Hamidson, H., Damiri, N., & Angraini, E. (2018). Effect of medicinal plants extracts on the incidence of mosaic disease caused by *Cucumber mosaic virus* and growth of chili. *IOP Conference Series: Earth and Environmental Science, 102*(1), Article 012062. https://doi.org/10.1088/1755-1315/102/1/012062

Hirata, S., Abdelrahman, M., Yamauchi, N., & Shigyo, M. (2016). Characteristics of chemical components in genetic resources of garlic *Allium sativum* collected from all over the world. *Genetic Resources and Crop Evolution, 63*(1), 35–45. https://doi.org/10.1007/s10722-015-0233-7

Hornickova, J., Kubec, R., Cejpek, K., Velisek, J., Ovesna, J., & Stavelikova, H. (2010). Profiles of *S*-alk(en)ylcysteine sulfoxides in various garlic genotypes. *Czech Journal of Food Sciences, 28*, 298–308. https://doi.org/10.17221/135/2010-CJFS

Ichikawa, M., Ide, N., & Ono, K. (2006). Changes in organosulfur compounds in garlic cloves during storage. *Journal of Agricultural and Food Chemistry, 54*(13), 4849–4854. https://doi.org/10.1021/jf060083o

Iobbi, V., Lanteri, A. P., Minuto, A., Santoro, V., Ferrea, G., Fossa, P., et al. (2022). Autoxidation products of the methanolic extract of the leaves of *Combretum micranthum* exert antiviral activity against *Tomato Brown Rugose Fruit Virus* (ToBRFV). *Molecules, 27*(3), 760. https://doi.org/10.3390/molecules27030760

Ipek, M., Ipek, A., & Simon, P. W. (2003). Comparison of AFLPs, RAPD markers, and isozymes for diversity assessment of garlic and detection of putative duplicates in germplasm collections. *Journal of the American Society for Horticultural Science, 128*(2), 246–252. https://doi.org/10.21273/jashs.128.2.0246

Islam, W., Adnan, M., Tayyab, M., Hussain, M., & Islam, S. U. (2018). Phyto-metabolites, an impregnable shield against plant viruses. *Natural Product Communications, 13*(1), 105–112.

Kodera, Y., Kurita, M., Nakamoto, M., & Matsutomo, T. (2020). Chemistry of aged garlic: Diversity of constituents in aged garlic extract and their production mechanisms via the combination of chemical and enzymatic reactions (review). *Experimental and Therapeutic Medicine, 19*(2), 1574–1584. https://doi.org/10.3892/etm.2019.8393

Kodera, Y., Ushijima, M., Amano, H., Suzuki, J.-I., & Matsutomo, T. (2017). Chemical and biological properties of *S*-1-propenyl-L-cysteine in aged garlic extract. *Molecules, 22*(4), 570. https://doi.org/10.3390/molecules22040570

Künstler, A., Gullner, G., Ádám, A. L., Kolozsváriné Nagy, J., & Király, L. (2020). The versatile roles of sulfur-containing biomolecules in plant defense - a road to disease resistance. *Plants, 9*(12). https://doi.org/10.3390/plants9121705

Lakoba, V. T., & Barney, J. N. (2020). Home climate and habitat drive ecotypic stress response differences in an invasive grass. *AoB PLANTS, 12*(6). https://doi.org/10.1093/aobpla/plaa062

Lanzotti, V. (2012). Bioactive polar natural compounds from garlic and onions. *Phytochemistry Reviews, 11*(2), 179–196. https://doi.org/10.1007/s11101-012-9247-3

Lawson, L. D., Wang, Z.-y. J., & Hughes, B. G. (1991). γ-Glutamyl-*S*-alkylcysteines in garlic and other *Allium* spp.: Precursors of age-dependent trans-1-propenyl

thiosulfinates. *Journal of Natural Products, 54*(2), 436–444. https://doi.org/10.1021/np50074a014

Liaqat, A., Zahoor, T., Atif Randhawa, M., & Shahid, M. (2019). Characterization and antimicrobial potential of bioactive components of sonicated extract from garlic (*Allium sativum*) against foodborne pathogens. *Journal of Food Processing and Preservation, 43*(5), Article e13936. https://doi.org/10.1111/jfpp.13936

Li, R., Baysal-Gurel, F., Abdo, Z., Miller, S. A., & Ling, K.-S. (2015). Evaluation of disinfectants to prevent mechanical transmission of viruses and a viroid in greenhouse tomato production. *Virology Journal, 12*(1), 5. https://doi.org/10.1186/s12985-014-0237-5

Lu, B., Taraporewala, F., Stubbs, G., & Culver, J. N. (1998). Intersubunit interactions allowing a carboxylate mutant coat protein to inhibit *Tobamovirus* disassembly. *Virology, 244*(1), 13–19. https://doi.org/10.1006/viro.1998.9099

Martins, N., Petropoulos, S., & Ferreira, I. C. F. R. (2016). Chemical composition and bioactive compounds of garlic (*Allium sativum* L.) as affected by pre- and post-harvest conditions: A review. *Food Chemistry, 211*, 41–50. https://doi.org/10.1016/j.foodchem.2016.05.029

Meier, U. (2018). *Growth stages of mono- and dicotyledonous plants - BBCH monograph Quedlinburg: Open Agrar Repositorium*.

Messiaen, C. M., Cohat, J., Leroux, J., Piechon, M., & Beyries, A. (1993). *Les allium alimentaires, reproduits par voie végétative*. Paris (France): Institut National de Recherche Agronomique (I.N.R.A.).

MIPAAF. (2021). Aggiornamento dell'elenco nazionale dei prodotti agroalimentari tradizionali ai sensi dell'articolo 12, comma 1, della legge 12 dicembre 2016, n. 238. (21A01168). In *Ministero delle politiche agricole alimentari e forestali (Ed.), Ventunesima revisione dell'elenco dei prodotti agroalimentari tradizionali (Vol. Serie Generale n.48 del 26-02-2021 - suppl. Ordinario n. 15)*. Rome, Italy: Gazzetta Ufficiale della Repubblica Italiana.

Montaño, A., Beato, V. M., Mansilla, F., & Orgaz, F. (2011). Effect of genetic characteristics and environmental factors on organosulfur compounds in garlic (*Allium sativum* L.) grown in Andalusia, Spain. *Journal of Agricultural and Food Chemistry, 59*(4), 1301–1307. https://doi.org/10.1021/jf104494j

Nakamoto, M., Fujii, T., Matsutomo, T., & Kodera, Y. (2018). Isolation and identification of three γ-glutamyl tripeptides and their putative production mechanism in aged garlic extract. *Journal of Agricultural and Food Chemistry, 66*(11), 2891–2899. https://doi.org/10.1021/acs.jafc.7b05480

Pooler, M. R., & Simon, P. W. (1994). True seed production in garlic. *Sexual Plant Reproduction, 7*(5), 282–286. https://doi.org/10.1007/BF00227710

Rabinkov, A., Miron, T., Mirelman, D., Wilchek, M., Glozman, S., Yavin, E., et al. (2000). *S*-allylmercaptoglutathione: The reaction product of allicin with glutathione possesses SH-modifying and antioxidant properties. *Biochimica et Biophysica Acta, 1499*(1–2), 144–153. https://doi.org/10.1016/s0167-4889(00)00119-1

Rouf, R., Uddin, S. J., Sarker, D. K., Islam, M. T., Ali, E. S., Shilpi, J. A., et al. (2020). Antiviral potential of garlic (*Allium sativum*) and its organosulfur compounds: A systematic update of pre-clinical and clinical data. *Trends in Food Science & Technology, 104*, 219–234. https://doi.org/10.1016/j.tifs.2020.08.006

Scholthof, K. B. (2004). *Tobacco mosaic virus*: A model system for plant biology. *Annual Review of Phytopathology, 42*, 13–34. https://doi.org/10.1146/annurev.phyto.42.040803.140322

Schrödinger. (2021). *Schrödinger release 2021: Maestro, Glide, Ligprep, Prime*. New Yourk, NY: Schrödinger, LLC.

Volk, G. M. (2009). Phenotypic characteristics of ten garlic cultivars grown at different North American locations. *Horticultural Science, 44*(5), 1238–1247.

Yuan, H., Sun, L., Chen, M., & Wang, J. (2016). The comparison of the contents of sugar, Amadori, and Heyns compounds in fresh and black garlic. *Journal of Food Science, 81*(7), 1–7. https://doi.org/10.1111/1750-3841.13365

Zhang, S., Griffiths, J. S., Marchand, G., Bernards, M. A., & Wang, A. (2022). *Tomato brown rugose fruit virus*: An emerging and rapidly spreading plant RNA virus that threatens tomato production worldwide. *Molecular Plant Pathology, 23*(9), 1262–1277. https://doi.org/10.1111/mpp.13229

Zhao, L., Zhang, J., Liu, T., Mou, H., Wei, C., Hu, D., et al. (2020). Design, synthesis, and antiviral activities of coumarin derivatives containing dithioacetal structures. *Journal of Agricultural and Food Chemistry, 68*(4), 975–981. https://doi.org/10.1021/acs.jafc.9b06861